

# Precipitation delivery in the tropical high Andes of southern Peru: new findings and paleoclimatic implications

L. B. Perry,<sup>a\*</sup> Anton Seimon<sup>b</sup> and Ginger M. Kelly<sup>a</sup>

<sup>a</sup> Department of Geography and Planning, Appalachian State University, Boone, NC, USA

<sup>b</sup> Wildlife Conservation Society, 2320 Southern Boulevard, Bronx, NY, USA

**ABSTRACT:** The Cordillera Vilcanota in the southern Peruvian Andes has been the site of significant research focused on paleoclimatic reconstructions from ice cores (Quelccaya), past glaciations, climate–glacier interactions, and ecological and human responses to climate change. In this article, we analyse precipitation patterns in the region from 2004 to 2010 using twice daily precipitation observations from six regional climate stations and hourly observations of precipitation intensity from nearby Cusco International Airport. We also analyse atmospheric fields of temperature, wind, and moisture at 700 and 200 hPa from the National Centers for Environmental Prediction/National Center for Atmospheric Research (NCEP/NCAR) reanalysis dataset and create 72-h antecedent upstream air trajectories for the heaviest precipitation events using the National Oceanic and Atmospheric Administration (NOAA) Hybrid Single Particle Lagrangian Integrated Trajectory (HYSPLIT) model. Results indicate that the majority of annual precipitation across the cordilleras and inter-montane valleys alike occurs from nocturnal, regionally coherent rainfall events, inferred to be stratiform in structure, that occur in association with deep moist convection over adjacent Amazon lowlands. Low-level moisture (as inferred from the antecedent upstream air trajectories) for precipitation events can be supplied from a number of different regions, including from the northwest and west. The trajectory analysis reveals a strong dominance (83%) of precipitation events occur under weak flow regimes from nearby Amazon basin source regions, with 50% associated with trajectories from the northwest. In addition, the El Niño–Southern Oscillation (ENSO) signal reported in previous work in the central Andes is not necessarily representative of the Cordillera Vilcanota, where La Niña years (including 2007–2008) typically experience slightly below normal precipitation and El Niño years (including 2009–2010) are considerably wetter. These results are of particular value in understanding atmospheric signals registered in Andean low latitude ice cores, and point the way towards obtaining greater climatological inference from parameters preserved in annual snow and ice stratigraphy.

**KEY WORDS** Cordillera Vilcanota; central Andes Mountains; precipitation; air trajectories; ENSO

Received 27 July 2012; Revised 4 January 2013; Accepted 16 January 2013

## 1. Introduction

Precipitation variability in tropical high mountains is a fundamental, yet poorly understood, factor influencing local climatic expression and glacier behaviour (Francou *et al.*, 2003; Kaser *et al.*, 2004; Barry, 2008; Chan *et al.*, 2008; Vuille, 2011). Precipitation phase (e.g. rain vs snow), timing, frequency, and amount control surface albedo, whereas cloud cover associated with precipitation events reduces solar radiation. As such, a decrease in precipitation (snowfall) is likely the primary factor driving the rapid deglaciation of equatorial high mountains in east Africa (Kaser *et al.*, 2004; Kaser *et al.*, 2010). Similarly, a delayed onset of the wet season, along with decreased precipitation, reduced cloud cover, and higher temperatures associated with the strong 1997–1998 El Niño event in the tropical Andes of Bolivia, resulted in the loss of one third of the total

volume of the Chacaltaya glacier (Francou *et al.*, 2003) and runoff from nearby Zongo glacier was two thirds higher than normal (Wagnon *et al.*, 2001). Tropical deglaciation is already impacting downstream human populations and impacts are projected to become more severe in coming decades (Chevallier *et al.*, 2011). It is also increasingly recognized (Vimeux *et al.* 2009; Kellerhals *et al.*, 2010) that precipitation variability is the dominant influence on stable oxygen isotope ratios ( $\delta^{18}\text{O}$ ) preserved in tropical ice cores, a critical yet incompletely understood paleoclimatic archive.

The rapidity of the climatic (Vuille, 2011), glaciological (Chevallier *et al.*, 2011), and ecological (Seimon *et al.*, 2007) changes observed in tropical high mountains points to the importance of improving understanding of precipitation processes and patterns as fundamental components of local and regional climatology. The purpose of this article is to therefore investigate precipitation patterns and delivery mechanisms in the Cordillera Vilcanota ( $\sim 14^\circ\text{S}$ ) of southern Peru (Figure 1) in the context of climate change, inter-annual climate variability, and interpretation of ice cores as tropical paleoclimatic archives.

\* Correspondence to: L. Baker Perry, Department of Geography and Planning, Appalachian State University, Boone, NC 28608, USA.  
E-mail: perrylb@appstate.edu

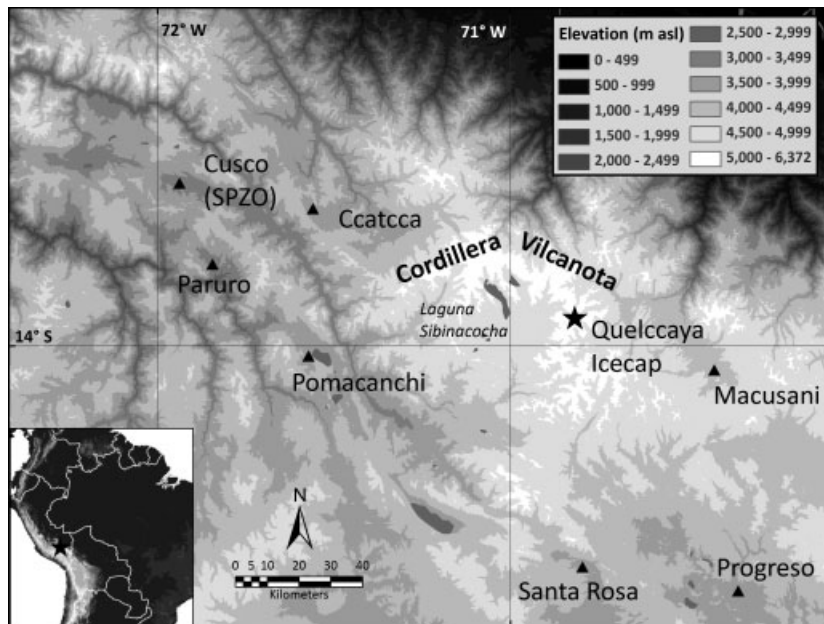


Figure 1. Topography and locations of precipitation observing stations used in this study in the Cordillera Vilcanota highlands region of southern Peru in the central Andes.

## 2. Literature synthesis

The Cordillera Vilcanota is one of the principal ranges in the Andes Mountains and home to the Quelccaya Icecap, the largest icecap in the tropics. Located approximately 80–130 km east-southeast of Cusco, the Cordillera Vilcanota has the second largest glacierized area in the tropics, behind only the Cordillera Blanca of northern Peru (Morales-Arnao, 1999). Six of its peaks reach above 6000 m above sea level, with Nevado Ausangate (6384 m) the highest. Likewise, the Cordillera Vilcanota is also home to the largest high alpine lake in the Andes, Laguna Sibinacoča (~30 km<sup>2</sup> at 4869 m), and source of the Vilcanota-Urubamba River, a critical water resource for hydroelectricity, irrigation, and tourism. Significant deglaciation is underway in the Cordillera Vilcanota (Seimon *et al.*, 2007), with reduction in ice cover area (volume) from 440 km<sup>2</sup> (17.0 km<sup>3</sup>) in 1962 to 297 km<sup>2</sup> (9.2 km<sup>3</sup>) in 2006 (Salzmann *et al.*, 2012), which is consistent with observations from elsewhere in the tropical Andes (Vuille *et al.*, 2008; Jomelli *et al.*, 2009).

Over the past several decades, the Cordillera Vilcanota has been the site of significant interdisciplinary research focused on three primary areas: paleoclimatic reconstruction, glaciology, and ecological responses to climate change. Glaciological investigations of past glaciations and glacier–climate interactions in the Cordillera Vilcanota have provided important findings on the timing, magnitude, and equilibrium line altitude (ELA) depressions of past glaciations (Thompson, 1980; Goodman *et al.*, 2001; Mark *et al.*, 2002) while other studies (Albert, 2002; Salzmann *et al.*, 2012) have investigated glacier change using remote sensing techniques. Recent research on ecological responses to climate change in the Cordillera Vilcanota has indicated that ongoing deglaciation has resulted in

the extension of the biosphere to extreme elevations (Seimon *et al.*, 2007). Amphibians, along with the pathogenic chytrid fungus, are now found above 5200 m in recently deglaciated terrain. Human land use patterns likewise indicate a response to moderating climatic conditions. The upper limit of potato cultivation has increased by several hundred meters over recent decades in the Cordillera Vilcanota to as high as 4550 m (Hole *et al.*, 2010).

The most significant research though relates to the Quelccaya ice cores, obtained by teams from Ohio State University in 1983 and 2003. These have yielded the longest annually resolvable ice core records in the tropics, including a detailed depiction of the Little Ice Age at seasonal resolution (Thompson *et al.*, 1985, 1986, 2006). The paleoclimatic interpretations remain somewhat uncertain given the subjective methodology and dating of the original cores (Seimon, 2003) and the recognized complexities of stable oxygen isotope ratios (deuterium and  $\delta^{18}\text{O}$ ) preserved in tropical Andean ice cores (NRC, 2006; Vimeux *et al.*, 2009; Kellerhals *et al.*, 2010). Precipitation processes (as opposed to temperature) are now recognized as playing a dominant, if highly complex, role in influencing the  $\delta^{18}\text{O}$  profiles preserved in tropical ice cores (Vimeux *et al.*, 2009; Kellerhals *et al.*, 2010). Regional coherence in decade-scale isotopic variability among Andean ice core sites has been demonstrated by the Andean Isotope Index (Hoffmann *et al.*, 2003), yet the exact mechanisms by which precipitation processes serve as the mediator between local climate and  $\delta^{18}\text{O}$  ratios preserved in seasonal snow and ultimately, in glacier ice, remain a challenge to understand. There is no single controlling factor that dominates the imprint of climate on isotopic ratios and, consequently, there is a need for a full understanding of local and regional dynamic factors controlling water isotopes (Vimeux *et al.*, 2009).

Nonetheless, with a highly resolved sub-annual stratigraphic record, extending back more than 1000 years, the Quelccaya ice core records are one of the most significant and widely used paleoclimatic proxies from the Neotropics, and present rich opportunities to comprehensively establish the relationship between isotopic signals and climatic conditions.

Another problematic aspect in deriving paleoclimatic inference from the ice cores is that understanding of meteorological factors contributing to precipitation at Quelccaya, and across the region more generally, is only partially known. Although it is widely recognized that precipitation variability is a fundamental influence on past and current changes in the tropical Andes (Francou *et al.*, 2003; Garreaud *et al.*, 2003; Bush *et al.*, 2010), only a small number of studies have focused explicitly on precipitation processes and patterns in the region. As far as we are aware, no study to date has investigated precipitation patterns in the Cordillera Vilcanota, despite the significant influence precipitation has on paleoarchives (especially ice cores), glacier behaviour, and ecology. From a glaciological perspective, precipitation type, amount, and timing control surface albedo, which are critical to glacier mass balance in the tropics (Francou *et al.*, 2003). Early and frequent snowfall during the wet season, which also coincides with the high-sun season in the central Andes (located between 10° and 30°S), maintains a high albedo on the glacier surface and effectively mitigates ablation of the glacial surface from intense solar radiation. A delayed start to the wet season, more sporadic precipitation, along with more liquid precipitation on the glacier surface, typically leads to rapid ablation of snow and ice (Francou *et al.*, 2003). Precipitation characteristics, such as the fraction of total precipitation falling as rain *versus* snow and precipitation timing and intensity, are also critical influences on basic ecological processes.

The central Andes are characterized by distinct seasonality of precipitation, with a wet season from November to March (shorter in the south and west) and a dry season from April through October. In the wet season, previous research has shown that easterly flow (at low levels and aloft) and upper-level divergence associated with the southward migration of an upper-tropospheric anticyclone, the Bolivian High (Lenters and Cook, 1997) often transports Amazonian moisture to the inter-Andean valleys, high cordilleras, and adjacent Altiplano (Garreaud, 1999; Garreaud and Aceituno, 2001). Due to high basal elevation and the high sun angle the troposphere typically becomes conditionally unstable on a daily basis throughout the year from diurnal heating. Consequently, Garreaud *et al.* (2003) suggest that the near-surface mixing ratio ( $Q_s$ ) is the critical ingredient for the development of precipitation. During periods when the  $Q_s$  exceeds a threshold value of  $5 \text{ g kg}^{-1}$ , deep, moist convection usually develops, resulting in abundant precipitation, as inferred from satellite retrievals of outgoing long-wave radiation (OLR). Moisture responsible for the wet periods in the Altiplano in 2002–2003 is observed to have

advected into the region from the east at the same altitude (Falvey and Garreaud, 2005). During the dry season, strong subsidence associated with the seasonal shift in the Hadley circulation along with enhanced upper-level westerly flow, largely prevents the transport of Amazonian moisture into the inter-Andean region. On occasion, tropospheric disturbances of extratropical origin associated with strong cold air outbreaks and upper-level cutoff lows during the dry season can also bring precipitation to the central Andean region, including snowfall across much of the Altiplano (Vuille and Ammann, 1997).

A central tenet of tropical Andean climatology is that most precipitation is convective in nature, predominantly occurring during the afternoon and early evening (Johnson, 1976; Aceituno, 1997; Garreaud *et al.*, 2003; Vuille and Keimig, 2004). The paucity of reliable networks of sub-daily precipitation observations has hindered investigations of the diurnal patterns of precipitation, as previous work has largely relied on OLR signatures. Cloud-top temperatures are inadequate indicators for confirming the presence of stratiform precipitation, particularly beneath cirrus shields, while space-borne radar has shown that contrary to expectations, significant stratiform precipitation occurs across tropical South America (Houze, 1997; Romatschke and Houze, 2010). In an analysis of convective cloudiness over the tropical and subtropical Americas, Garreaud and Wallace (1997) further note that ‘the frequency of cold (<235 K) clouds may be biased towards late afternoon/early evening, relative to associated precipitation.’ In fact, Garreaud (1999) notes that considerable cold cloud cover (<235 K) remains over the Altiplano between 00 and 06 UTC [19–01 Local Standard Time (LST)] during rainy episodes. Although the accuracy of satellite-borne radar observations [Tropical Rainfall Measuring Mission (TRMM)] in the tropical high Andes is questionable at finer temporal scales (Scheel *et al.*, 2011), recent results furthermore indicate that a substantial fraction of reflectivity signatures across the northeastern region of the central Andes, which encompasses the Cordillera Vilcanota region, are indicative of stratiform precipitation (Romatschke and Houze, 2010). Likewise, TRMM analyses from the Andean region (Biasutti *et al.*, 2011) show a nocturnal maximum in the timing of precipitation. Therefore, the prevailing view that central Andean precipitation is predominantly or even exclusively (Vuille and Keimig, 2004) convective and occurring in the late afternoon and early evening hours needs to be reconsidered and evaluated with quantitative data from individual precipitation events.

Inter-annual variability of precipitation in the tropical Andes is strongly controlled by tropical Pacific sea-surface temperatures (SSTs) and associated El Niño–Southern Oscillation (ENSO). Vuille (1999) found that during the cold-phase of ENSO (La Niña), easterly flow and associated Amazonian moisture transport during the wet season is enhanced, resulting in above normal precipitation, greater cloud cover, and lower temperatures in the central Andes. During the warm-phase of ENSO (El Niño), enhanced upper-level westerly flow leads to

a delay in the onset of the wet season. In addition, the central Andes experience below normal precipitation and associated reductions in cloud cover (Vuille and Keimig, 2004) and higher temperatures (Vuille *et al.*, 2003). Consequently, several studies (Wagnon *et al.*, 2001; Francou *et al.*, 2003) have reported rapid glacier ablation and highly negative mass balance during strong El Niño events, such as 1997–1998.

Despite the significant recent advances in understanding the basic climatology and physical processes associated with precipitation across the tropical Andes, numerous uncertainties remain. In particular, the timing (diurnal *vs* nocturnal), spatial extent, proportion of convective *versus* stratiform events and intensity of precipitation events remain poorly understood. While a robust relationship between tropical Pacific SSTs and atmospheric circulation (strongly related to ENSO as discussed previously) over the tropical Andes has been established at seasonal, annual, and inter-annual time scales, it remains unclear how much intra-seasonal variability exists, particularly associated with individual precipitation events. Likewise, the degree of variability within the antecedent upstream air trajectories associated with precipitation events has not been investigated. Finally, it is unclear whether the results obtained from previous work in the central Andes (especially the Peru-Bolivia Altiplano) are representative of the Cordillera Vilcanota. Vuille and Keimig (2004) suggest that the spatial variability of precipitation across the central Andes is higher than previously thought and that the geographic complexity of the regional climate needs further investigation. Taken together, these uncertainties have sustained limitations on the climatological inference derived from Quelccaya and other ice core data series obtained from across the central Andean region. Furthermore, understanding regional variability in climate and precipitation is particularly important to interpreting local implications of precipitation changes projected by climate models incorporating anthropogenic greenhouse gas increases (Urrutia and Vuille, 2009).

In this article, we utilize high temporal resolution observations to investigate precipitation patterns in the Cordillera Vilcanota of Peru for the period 2004–2010. Our work is motivated by uncertainties associated with precipitation delivery mechanisms in the context of contemporary climate change and in the existing interpretations of the Quelccaya ice cores. The analysis is guided by three major research questions: (1) Is there regional coherency in precipitation timing and amount for climate stations surrounding the Cordillera Vilcanota? (2) What are the dominant antecedent 72-h upstream air trajectories associated with precipitation events? and (3) How does ENSO phase (El Niño *vs* La Niña) influence precipitation patterns in the Cordillera Vilcanota?

### 3. Data and methods

Precipitation data were obtained from the Peruvian National Meteorology and Hydrology Service

(SENAMHI) as well as from METAR observations from Cusco's Jorge Velasco International Airport (SPZO) for the period 1 August 2004 to 31 July 2010 (Table 1). The SENAMHI precipitation data were accessed directly from the SENAMHI website (SENAMHI, 2010) and consist of twice daily manual precipitation observations (0700 and 1900 LST; LST = UTC-5 h), providing the opportunity to quantify the fraction of 24-h total precipitation occurring during daytime (diurnal) *versus* night-time (nocturnal) hours. The METAR hourly precipitation data were obtained from various archival sources, including the National Center for Atmospheric Research (NCAR) surface weather page (NCAR, 2010) and Plymouth State University.

Hourly precipitation data from Cusco (SPZO) were summed to derive twice daily totals for comparison with the SENAMHI precipitation data and were also used to identify 847 separate precipitation events during the period of study. We defined the beginning of a precipitation event as the hour measurable precipitation was first reported, the maturation of the event as the hour with the highest precipitation total, and the ending as the last hour measurable precipitation occurred. A precipitation event remained active if measurable precipitation was reported during a 6-h period; precipitation breaks over 6 h resulted in the identification of separate precipitation events.

The National Oceanic and Atmospheric Administration (NOAA) Hybrid Single Particle Lagrangian Integrated Trajectory (HYSPLIT) Model (Draxler and Hess, 1998; Draxler and Rolph, 2011) was used to simulate 72-h backward air trajectories ending at the maturation date and time of each event. The coordinate location of Cusco (SPZO) was used as the trajectory ending location (13.5357°S, 71.9388°W), and each trajectory was developed using an ending elevation of 4000 m, or approximately 600 hPa. The 600 hPa level is a common cloud base height during precipitation events over Cusco and is therefore a representative end point for investigating antecedent upstream air trajectories and associated transport of low-level moisture.

HYSPLIT backward trajectories were derived using four-dimensional ( $x$ ,  $y$ ,  $z$ ,  $t$ ) meteorological fields from the Global Data Analysis System (GDAS) dataset (NOAA, 2011). GDAS data are available from 2004 at three-hourly temporal resolution and one-degree (latitude/longitude grid) spatial resolution with 23 vertical levels. For periods of missing GDAS data (~4 weeks or 1.3% of the study period), the 2.5-degree National Centers for Environmental Prediction/National Center for Atmospheric Research (NCEP/NCAR) reanalysis data (Kalnay *et al.*, 1996) were used. Previous work (Perry *et al.*, 2007) suggests that the NCEP/NCAR reanalysis data compare favourably to higher resolution datasets in eastern North America when used for 72-h antecedent upstream air trajectory analyses. Some uncertainty likely exists in the Reanalysis data given the paucity of upper-air and surface observations in South America and especially in the central Andes.

Table 1. Summary of data sources.

| Variables                 | Temporal resolution      | Period    | Source                    |
|---------------------------|--------------------------|-----------|---------------------------|
| Precipitation             | 1 h                      | 2004–2010 | Cusco Airport (SPZO)      |
| Backward air trajectories | 1 h                      | 2004–2010 | NOAA HYSPLIT Model        |
| Synoptic fields           | 6 h                      | 2004–2010 | NCEP/NCAR reanalysis      |
| Precipitation             | 12 h (0700 and 1900 LST) | 2004–2010 | SENAMHI climate stations  |
| Precipitation             | 24 h (2400 LST)          | 1963–2009 | Cusco University (UNSAAC) |

We performed a cluster analysis of all the HYSPLIT backward air trajectories associated with the maturation hour of precipitation events in Cusco from 2004 to 2010. In addition, we clustered trajectories from all precipitation events during the 2007–2008 La Niña and the 2009–2010 El Niño. This approach was based on the clustering methodology used by Taubman *et al.* (2006), in which similar trajectories are combined into groups or clusters, maximizing the differences in clusters of trajectories. Each cluster therefore should represent different synoptic regimes and source regions influencing the entire sample of trajectories. In HYSPLIT, clusters of trajectories are created by calculating the total spatial variance (TSV) through multiple iterations. When TSV is compared to the total numbers of clusters, the step just before the large increase in TSV suggests an ideal final number of clusters. Although there is some subjectivity involved in choosing the number of clusters to use in the cluster analysis, the large change in TSV provides some objective guidance to the process and the final choice is not arbitrary (Taubman *et al.*, 2006). Composite synoptic plots of 700 and 200 hPa wind speed and direction for the heaviest precipitation events (top decile) in each trajectory cluster were also created from the NOAA-ESRL Physical Sciences website (NOAA-ESRL, 2011) using the NCEP/NCAR reanalysis data (Kalnay *et al.*, 1996).

For longer-term historical reference on ENSO-related precipitation variability we analysed additional precipitation data from 1963 to 2009 recorded at a university in Cusco [Universidad Nacional de San Antonio Abad del Cusco (UNSAAC)]. This station is located about 3 km and 117 m higher in elevation (3365 m) than SPZO. Daily precipitation data were summed into July to June hydrological year totals and then composited according to the corresponding austral summer Multivariate ENSO Index (MEI) means.

## 4. Results

### 4.1. Regional coherence in precipitation totals

Mean annual precipitation at highland climate stations near the Cordillera Vilcanota ranged from 560 to 857 mm for the period 2004–2010, with a regional mean of 697 mm (Table 2). The site at Progreso, located in the semi-arid northern Altiplano at 3965 m, was considerably drier than the other stations. In general, lower elevation valley stations (e.g. Paruro) exhibit

greater inter-annual variability of precipitation than at higher elevation stations (e.g. Macusani and Ccatcca) as indicated by the coefficients of variation (CV) (Table 2). Consistent with previous work (Garreaud *et al.*, 2003) and current understanding of central Andean climate, over half of the mean annual precipitation occurred during the climatological austral summer of December, January, and February (DJF). In contrast, the June to August climatological austral winter is normally quite dry, with only 1–2% of the mean annual total falling during this period.

Regional coherence in precipitation is also evident from the number of stations reporting precipitation during a given 12-h observation period (Table 3). It is relatively uncommon (13% of observations) for precipitation to only be observed at one station. Nearly all these observations are light (<0.39 mm or in the bottom quartile), suggesting that the precipitation may be associated with isolated convective activity. Approximately 60% of the time, five or more stations display coherence in their observations when all observations are analysed. This agreement increases substantially when only the top decile (i.e. heaviest 10%) of precipitation observations is included, with coherence occurring 85% of the time with five or more stations. This is consistent with studies from the greater Altiplano region to the south and west of the Cordillera Vilcanota that show that wet season precipitation is highly episodic, occurring across broad areas in multi-day periods alternating with dry conditions as air masses with high precipitable water content advect into the region and then become depleted by precipitation delivery (Garreaud, 2000; Falvey and Garreaud, 2005). Good regional coherence in the inter-annual variability of precipitation across the region is also evident (Figure 2), with all stations mostly varying in phase and exhibiting sharp increases between the 2008–2009 La Niña and the 2009–2010 El Niño events.

### 4.2. Precipitation timing

The SENAMHI observations provide an opportunity to analyse the fraction of mean annual precipitation that occurred at night *versus* day during the period of study (Table 4). Our results clearly show that most precipitation occurrence is nocturnal. This is especially the case for the heavier (top quartile) and heaviest (top decile) 12-h precipitation totals, with 75–85% of their respective contributions occurring nocturnally. Frequency histograms for the hourly precipitation data from SPZO illustrate the timing of precipitation events is bimodal,

Table 2. Mean annual precipitation and percent by season, 2005–2010 hydrological years.

| Station              | Elevation (m) | Percent complete | Mean annual precipitation (mm) | Standard deviation | Coefficient of variation | Percent of precipitation by season |           |          |           |
|----------------------|---------------|------------------|--------------------------------|--------------------|--------------------------|------------------------------------|-----------|----------|-----------|
|                      |               |                  |                                |                    |                          | DJF                                | MAM       | JJA      | SON       |
| Cusco                | 3249          | 100              | 631                            | 98                 | 15.6                     | 57                                 | 21        | 1        | 20        |
| Ccattcca             | 3729          | 99               | 670                            | 79                 | 11.7                     | 55                                 | 22        | 2        | 22        |
| Macusani             | 4331          | 99               | 623                            | 58                 | 9.4                      | 58                                 | 21        | 1        | 20        |
| Paruro               | 3084          | 99               | 788                            | 165                | 21.0                     | 56                                 | 22        | 1        | 21        |
| Pomacanchi           | 3200          | 99               | 857                            | 133                | 15.5                     | 52                                 | 24        | 1        | 23        |
| Progreso             | 3965          | 100              | 560                            | 78                 | 13.9                     | 57                                 | 21        | 1        | 21        |
| Santa Rosa           | 3940          | 98               | 752                            | 116                | 15.4                     | 57                                 | 22        | 1        | 19        |
| <i>Regional Mean</i> | <i>3643</i>   | <i>99</i>        | <i>697</i>                     | <i>94</i>          | <i>13.0</i>              | <i>55</i>                          | <i>22</i> | <i>1</i> | <i>21</i> |

Table 3. Percentage of SENAMHI stations reporting measurable ( $\geq 0.1$  mm) precipitation during each 12-h observing period.

| Number of stations reporting precipitation | All observations ( $n = 4382$ ) (%) | Bottom quartile ( $< 0.39$ mm) (%) | Top quartile ( $> 2.39$ mm) (%) | Top decile ( $> 4.55$ mm) (%) |
|--|-------------------------------------|------------------------------------|---------------------------------|-------------------------------|
| 0  | 50                                  |                                    |                                 |                               |
| 1  | 13                                  | 73                                 | 1                               | 0                             |
| 2  | 10                                  | 23                                 | 3                               | 0                             |
| 3  | 8                                   | 4                                  | 10                              | 2                             |
| 4  | 7                                   | 0                                  | 21                              | 12                            |
| 5  | 5                                   | 0                                  | 27                              | 23                            |
| 6  | 4                                   | 0                                  | 24                              | 33                            |
| 7  | 2                                   | 0                                  | 15                              | 29                            |

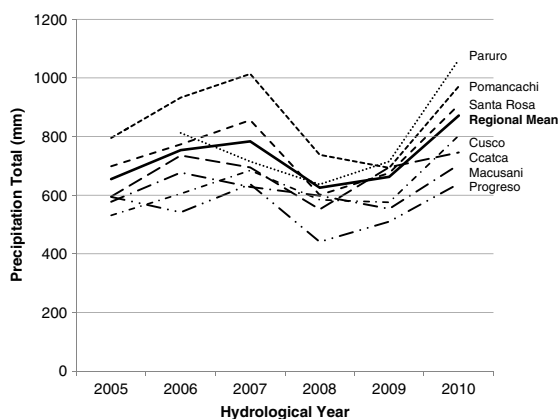


Figure 2. Hydrological year (August to July; years are labelled by the latter portion of the period) precipitation totals for climate stations in the Cordillera Vilcanota, 2005–2010.

with a pronounced late afternoon maximum occurring at 21 UTC (16 LST) and a broader nocturnal maximum evident from approximately 04 to 09 UTC (23–04 LST) (Figure 3). The hourly precipitation data also confirm that the heavy precipitation events (top quartile) occur almost exclusively at night, peaking around 05 UTC (00 LST).

The significance of nocturnal precipitation, particularly for the heavy events, identified in this study brings into question the widely held assertion that central Andean precipitation is tied to the release of convective instability that develops from diurnal heating in the presence of sufficient boundary layer moisture. Across the Cordillera Vilcanota region, we show that the pluvial maximum occurs close to local midnight (Figure 3),

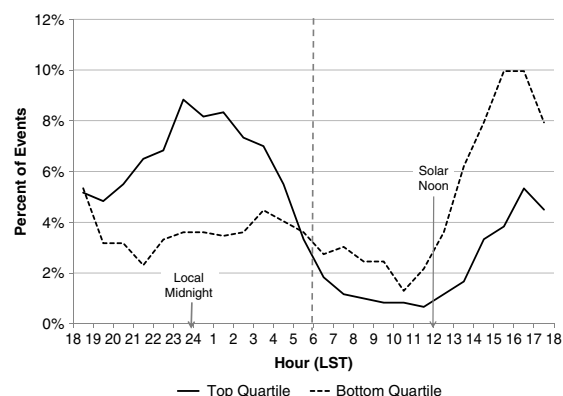


Figure 3. Temporal distribution of event maturation, the hourly period of highest precipitation rate shown in Local Standard Time (LST), for all precipitation events (upper) and top ( $> 5.8$  mm) versus bottom ( $< 0.7$  mm) quartiles of precipitation events (lower) at Cusco. Vertical dashed line in both panels indicates approximate time of local sunrise.

and is associated with long-duration events, often lasting through much of the night. Examination of 10 years of hourly synoptic METAR reports from SPZO indicates that observations of thunder accompanying precipitation around local midnight are almost non-existent, even at rainfall rates of up to  $9 \text{ mm h}^{-1}$  (not shown). Along with the timing being far removed from the period of diurnal heating, this also points to the improbability that these precipitation events are locally driven by convective updrafts in a low static stability environment. Without ground-based meteorological radar observations this is difficult to confirm; however, new analysis results from the space-borne TRMM radar appear to support

Table 4. Daily fraction of precipitation between 0700 and 1900 LST (diurnal) and 1900 and 0700 LST (nocturnal).

| Station              | Percent of annual mean |           | Percent of top quartile (>2.39 mm) |           | Percent of top decile (>4.55 mm) |           |
|----------------------|------------------------|-----------|------------------------------------|-----------|----------------------------------|-----------|
|                      | Nocturnal              | Diurnal   | Nocturnal                          | Diurnal   | Nocturnal                        | Diurnal   |
| Cusco                | 68                     | 32        | 75                                 | 25        | 86                               | 14        |
| Ccattcca             | 67                     | 33        | 77                                 | 23        | 88                               | 12        |
| Macusani             | 49                     | 51        | 64                                 | 36        | 81                               | 19        |
| Paruro               | 67                     | 33        | 74                                 | 26        | 87                               | 13        |
| Pomacanchi           | 69                     | 31        | 77                                 | 23        | 88                               | 12        |
| Progreso             | 72                     | 28        | 87                                 | 13        | 87                               | 13        |
| Santa Rosa           | 62                     | 38        | 78                                 | 22        | 84                               | 16        |
| <i>Regional Mean</i> | <i>65</i>              | <i>35</i> | <i>75</i>                          | <i>25</i> | <i>86</i>                        | <i>14</i> |

this conclusion for the broader region of the Andes encompassing the Cordillera Vilcanota (Romatschke and Houze, 2010).

#### 4.3. Antecedent upstream air trajectories

Results of the cluster analysis of the 72-h backward trajectories for precipitation events observed at Cusco suggest that approximately 83% of precipitation events occur under weak ( $\leq 1.04 \text{ m s}^{-1}$ ) low-level flow, while 95% of events are associated with low-level flow originating from the Amazon basin (Figures 4 and 5 and Table 5). Likewise, 50% of the precipitation events are associated with weak north-northwest flow (Cluster 1 in Figure 5) and an additional 8% of events exhibit back trajectories out of the north-northwest under stronger flow regimes (Cluster 5), with a mean advection rate of  $3.06 \text{ m s}^{-1}$ . Only one of the six composite trajectories (Cluster 6) does not originate over the Amazon basin, thus confirming the importance of Amazonian moisture to modern climate across the Cordillera Vilcanota and adjacent central Andean region. The average precipitation totals per event display remarkably little variability, ranging from 3.8 to 4.9 mm for clusters 1–5 (i.e. those with an Amazonian connection), with mean event durations ranging from 4.2 to 6.0 h.

The average precipitation (4.8 mm) associated with Cluster 6, which has an apparent connection to the Pacific Ocean, is higher than all the other trajectory clusters except Clusters 1 (4.9 mm) and 3 (4.8 mm). Interestingly, three of the events in Cluster 6 produced >25 mm of precipitation, and 72-h antecedent upstream air trajectories indicate that air parcels within the moist layer were likely near the surface of the Pacific Ocean 72 h before the event (Figure 6). One of these precipitation events (25.7 mm on 26 January 2010), along with very wet antecedent conditions, contributed to the flood of record on the Vilcanota/Urubamba Rivers (NOAA, 2010) and considerable societal impacts (Bulmer and Farquhar, 2010). The heavy precipitation associated with Cluster 6 is particularly surprising since Cusco and the Vilcanota are subject to downslope flow from higher terrain to the south-southwest, whereas the other clusters are tied to upslope flow from the Amazon Basin (Figure 7).

To highlight some of the salient synoptic patterns associated with the trajectory clusters, we created composite

plots of wind speed and direction at 700 and 200 hPa for the top decile of precipitation events at SPZO (Figure 8). For Cluster 1, a corridor of north-northwest flow parallel to the Andes at 700 hPa is evident and consistent with the composite trajectory (refer to Figure 5); this trajectory appears to parallel the western margin of the entrance region of the South American Low-Level Jet (Vera *et al.*, 2006). At 200 hPa, the Bolivian High is clearly evident despite a light flow regime. Very weak 700 hPa flow out of the north or north-east is evident for Cluster 3 and consistent with the composite trajectory. The Bolivian High is also evident at 200 hPa, although with much weaker flow across all tropical South America. For Cluster 6, a weak flow regime is also evident over southern Peru at 200 hPa, with a readily discernible Bolivian High. The composite plots highlight the weak flow associated with the heaviest precipitation events in each of the three trajectory clusters, while also clearly indicating that the low-level flow (and associated moisture source regions) can vary considerably even with similar manifestations of the Bolivian High. These results further reinforce the need for more detailed, process-oriented, investigations of central Andean precipitation events.

Although most of the trajectory clusters do not deviate considerably from the overall percent of diurnal *versus* nocturnal precipitation (Table 5), two deserve further commentary. Cluster 5, associated with north-northwest flow initially parallel to the eastern slopes of the Andes, exhibits a higher percentage of nocturnal precipitation events (75%) than the other clusters. Likewise, the southerly Cluster 6 also exhibits a significant nocturnal bias, with 67% of precipitation events occurring at night. From a seasonal perspective (Table 5), Clusters 5 and 6 are also somewhat anomalous when compared to the other trajectory clusters. Nearly half (43%) of the precipitation events in Cluster 5 occurred during the austral climatological spring (SON), considerably higher than the other clusters. In contrast, precipitation events in Cluster 6 mostly occurred (81%) during the austral climatological summer (DJF).

#### 4.4. ENSO influences on precipitation patterns

The La Niña of 2007–2008 and El Niño of 2009–2010 also provided an opportunity to assess the variability of

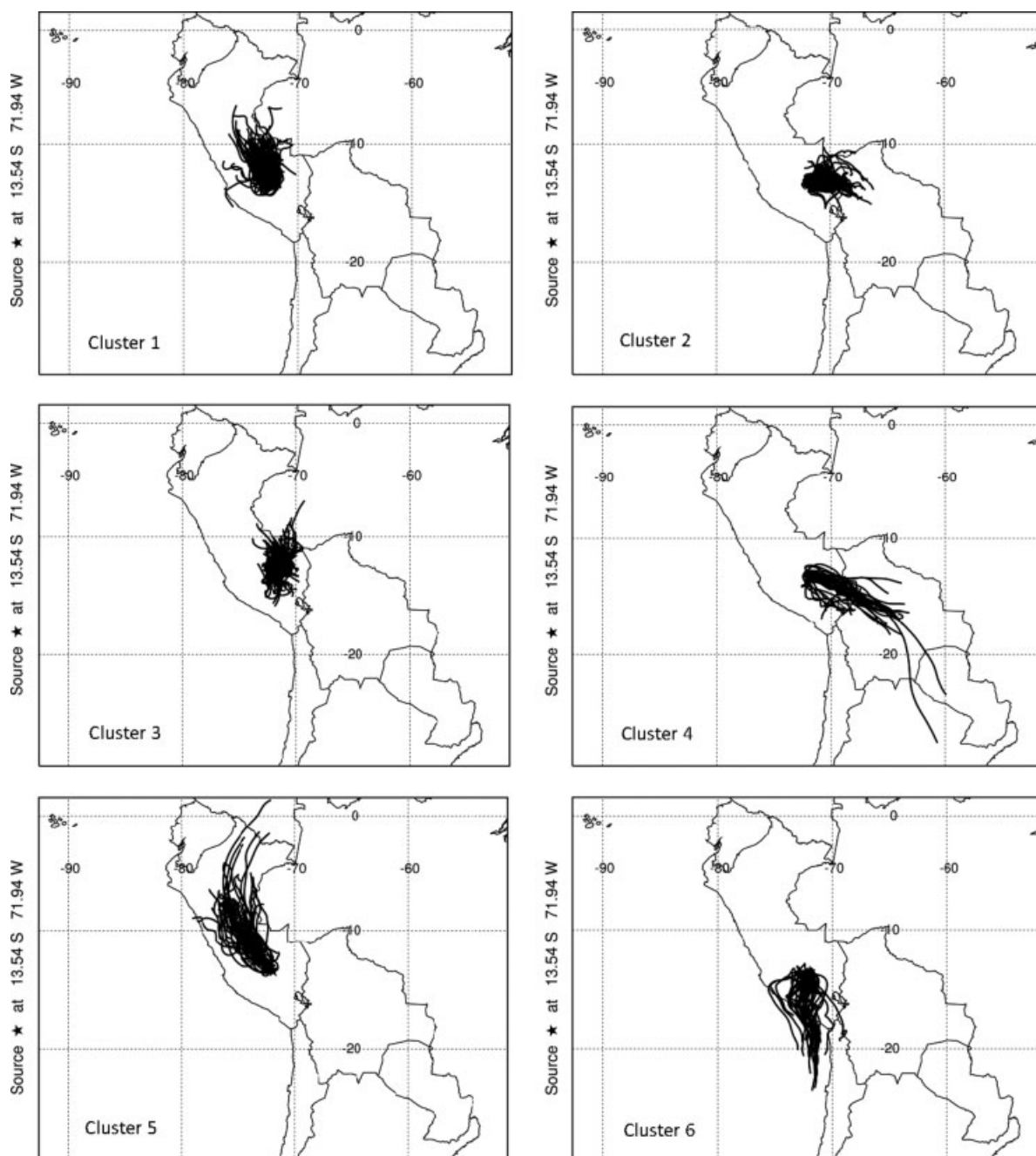


Figure 4. Hybrid Single Particle Lagrangian Integrated Trajectory (HYSPPLIT) 72-h backward air trajectory clusters and associated spaghetti plots for precipitation events at Cusco between 2004 and 2010: Cluster 1 (top left), Cluster 2 (top right), Cluster 3 (middle left), Cluster 4 (middle right), Cluster 5 (bottom left), and Cluster 6 (bottom right).

precipitation totals and associated upstream air trajectories across the Cordillera Vilcanota. La Niña conditions persisted for much of 2007 through 2009, reaching a minimum value of  $-1.6$  on the MEI (Wolter and Timlin, 1993) in February to March 2008; this ranks it as the third strongest at this time of year for the period 1950–2012 (NOAA, 2012). The 2009–2010 El Niño was comparably strong of the opposite sign, peaking with an MEI of  $+1.5$  early in 2010, ranking it as fourth strongest at the time of year. These events provide an opportunity to contrast the precipitation patterns and salient aspects of atmospheric circulation between hydrological

years characterized by opposite phases of ENSO. Total observed precipitation during the 2008 hydrological year (i.e. July 2007 to June 2008) in association with La Niña conditions was slightly below the 6-year mean (2005–2010 hydrological years) in Cusco ( $-4\%$ ) and the wider Vilcanota region ( $-14\%$ ), and considerably less than observed totals during 2010 hydrological year and the associated El Niño when observed precipitation was 20–32% above the 6-year mean in Cusco and the wider Vilcanota region (Table 6). Very little difference in the seasonal distribution of precipitation totals is evident between the two years.

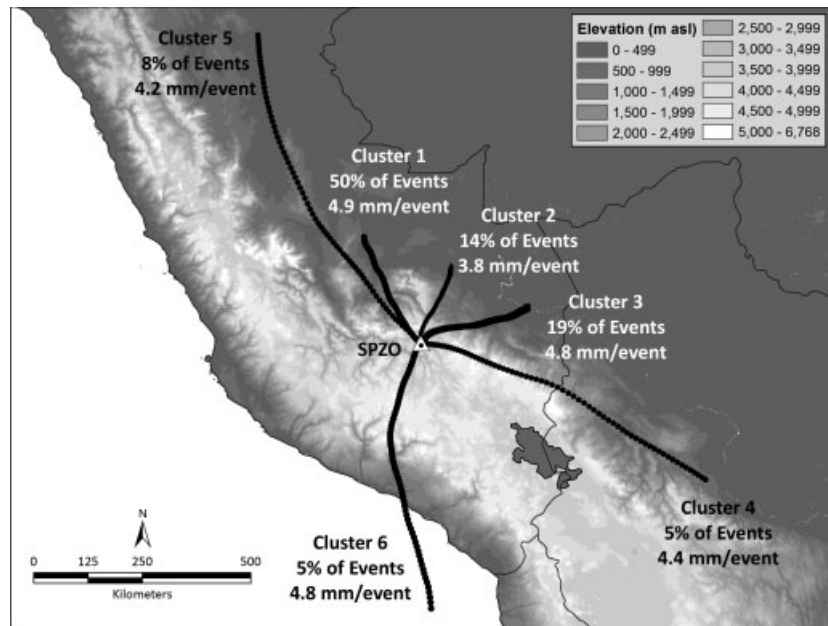


Figure 5. Composite 72-h HYSPLIT trajectory clusters plotted each hour and overlaid on topography for all for precipitation events observed at Cusco (SPZO) from August 2004 through July 2010.

Table 5. Precipitation characteristics associated with each trajectory cluster.

| Cluster     | Amount per event (mm) | Percent of total events | Percent of total precipitation | Mean duration (h) | Advection rate ( $m s^{-1}$ ) | Percent   |         | Percent by cluster |     |     |     |
|-------------|-----------------------|-------------------------|--------------------------------|-------------------|-------------------------------|-----------|---------|--------------------|-----|-----|-----|
|             |                       |                         |                                |                   |                               | Nocturnal | Diurnal | DJF                | MAM | JJA | SON |
| Cluster 1   | 4.9                   | 50                      | 52                             | 5.3               | 1.04                          | 53        | 47      | 53                 | 38  | 58  | 63  |
| Cluster 2   | 3.8                   | 14                      | 11                             | 4.7               | 0.71                          | 52        | 48      | 10                 | 19  | 17  | 8   |
| Cluster 3   | 4.8                   | 19                      | 19                             | 5.1               | 0.98                          | 63        | 37      | 16                 | 34  | 16  | 13  |
| Cluster 4   | 4.4                   | 5                       | 4                              | 6.0               | 2.68                          | 62        | 38      | 4                  | 4   | 0   | 5   |
| Cluster 5   | 4.2                   | 8                       | 7                              | 4.2               | 3.06                          | 57        | 43      | 7                  | 1   | 9   | 11  |
| Cluster 6   | 4.8                   | 5                       | 5                              | 4.8               | 2.34                          | 50        | 50      | 8                  | 1   | 0   | 0   |
| Unclustered | 4.4                   | <1                      | 2                              | 4.2               | –                             | 58        | 42      | 2                  | 1   | 0   | 0   |

A comparison of backward air trajectories associated with precipitation events between the 2007–2008 La Niña and the 2009–2010 El Niño years (Figure 9 and Table 7) illustrates some notable differences. In 2007–2008, approximately 45% of the precipitation events were tied to trajectories out of the N (Cluster LN1) and E (Cluster LN3), with 47% of the events tied to trajectories out of the NNW (Cluster LN2) (Figure 9(b)). In 2009–2010, however, only 30% of the precipitation events are tied to trajectories originating to the N and E of Cusco (Cluster EN2) and 64% of the events are characterized by backward air trajectories originating to the NNW and NW (Clusters EN1 and EN3) (Figure 9(b)). These results indicate that NNW and NW trajectories were clearly more numerous during the 2009–2010 El Niño year for two reasons: (1) the overall number of precipitation events was higher, and (2) the percentage of the total number of events tied to NNW and NW trajectories was much higher.

Composite plots of 700 and 200 hPa vector wind (Figure 10) for the climatological austral summer (DJF)

indicate that the 2007–2008 La Niña was characterized by weak E flow at 200 hPa and N or NW flow at 700 hPa. The 200 hPa flow during the 2009–2010 El Niño, however, displayed somewhat weaker E flow, with stronger NW flow at 700 hPa. These plots suggest that the synoptic environment during the 2007–2008 La Niña favoured moisture advection from the E and NE (e.g. stronger E and NE flow at 500 hPa) and that this flow weakened somewhat during the 2009–2010 El Niño. The NW flow at 700 hPa was also considerably stronger during the 2009–2010 El Niño, which helps to account for the high frequency of backward trajectories out of the NNW and NW during precipitation events. As noted previously, the regional landform morphology provides an avenue for Amazonian moisture to be transported into Cusco and the Cordillera Vilcanota not only out of the E and NE but also from the NW. Therefore, the synoptic conditions favouring NW flow at 700 hPa (and weak W flow at 500 hPa, not shown) during the 2009–2010 El Niño resulted in much above normal precipitation and more frequent precipitation events.

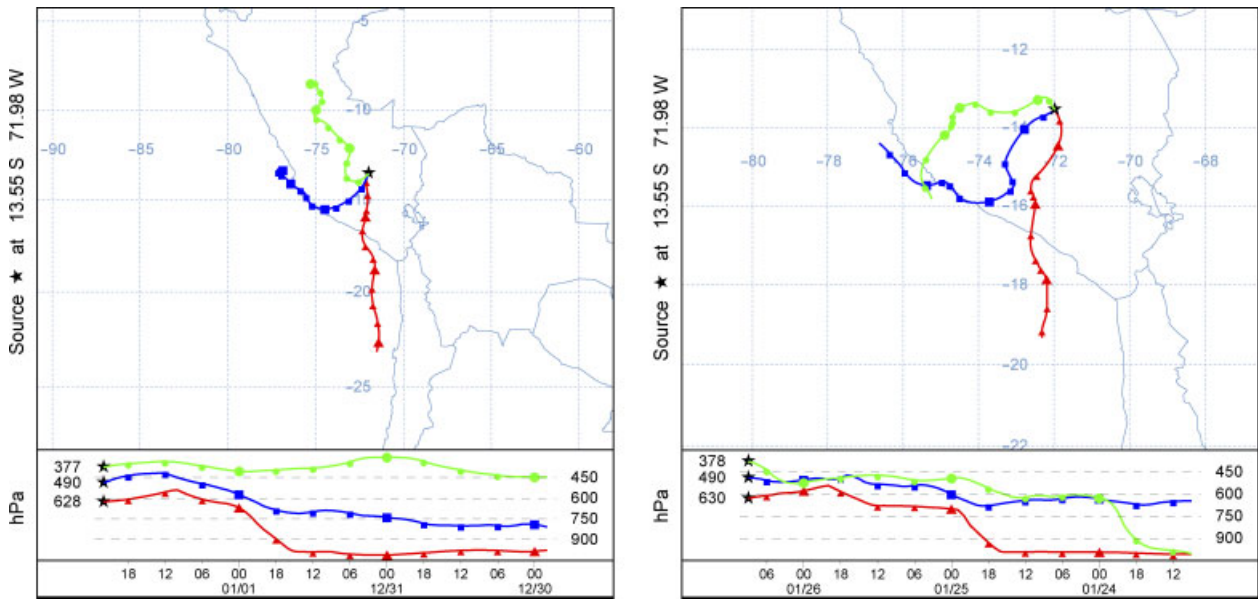


Figure 6. HYSPLIT analysis of 72-h backward air trajectories ending at 2200 UTC 1 January 2006 (left) and 0900 UTC 26 January 2010 (right) created using 1-degree spatial resolution Global Data Analysis System (GDAS) 3-hourly archive data.

Table 6. Precipitation characteristics during the 2007–2008 La Niña and the 2009–2010 El Niño.

| Year      | Cusco (SPZO)          |              |                  | 7-Station regional mean |              | Seasonal total (%) |     |     |     |
|-----------|-----------------------|--------------|------------------|-------------------------|--------------|--------------------|-----|-----|-----|
|           | Aug to Jul total (mm) | Anomaly (mm) | Number of events | Aug to Jul total (mm)   | Anomaly (mm) | SON                | DJF | MAM | JJA |
| 2007–2008 | 608                   | –23          | 131              | 641                     | –56          | 22                 | 57  | 19  | 2   |
| 2009–2010 | 834                   | 203          | 161              | 871                     | 174          | 23                 | 58  | 19  | 1   |

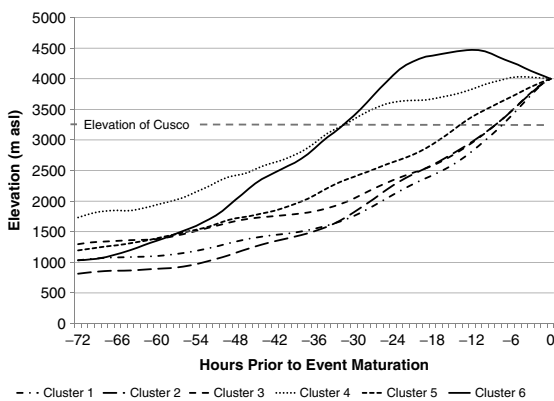


Figure 7. Vertical profiles of trajectory clusters (as presented in Figure 5) for precipitation events at Cusco between 2004 and 2010.

Due to the limitation of only examining one ENSO event of each type, this study cannot confirm whether these synoptic patterns are representative of other El Niño and La Niña years. Our results, however, may explain why many El Niño years are wet and La Niña years are dry in Cusco and the Cordillera Vilcanota (Figure 11). The hydrological year difference in precipitation accumulation at SPZO for the two strong ENSO events quantified in this study is 228 mm. Close to SPZO, at the Cusco university during the 47-year period 1963–2009, which

does include these two events, the hydrological year precipitation totals average 81 mm higher during strong El Niño events (December to March mean MEI > 1.0;  $n = 6$  events) when compared with strong La Niña events (December to March mean MEI < –1.0;  $N = 6$  events) (Figure 11). Most of the difference develops early in the wet season: between 1 November and 1 December the El Niño series averages 2 mm wetter per day than the La Niña series. Interestingly, mean daily precipitation totals vary out of phase during several periods at the height of the wet season, and the strong La Niñas feature much larger intra-seasonal variability during the December to March wet season peak. Differences in mean daily precipitation totals are smallest during dry months both preceding and following the November to April highly pluvial period.

### 5. Discussion

By referencing a complete dataset of individual precipitation events over a 6-year period, this study offers an opportunity to examine some of the fundamental characteristics of precipitation delivery for the Cordillera Vilcanota, one of the most significant glacierized mountain ranges of the tropics, and the Quelccaya Ice Cap, one of the most important paleoclimate sites. Much of the

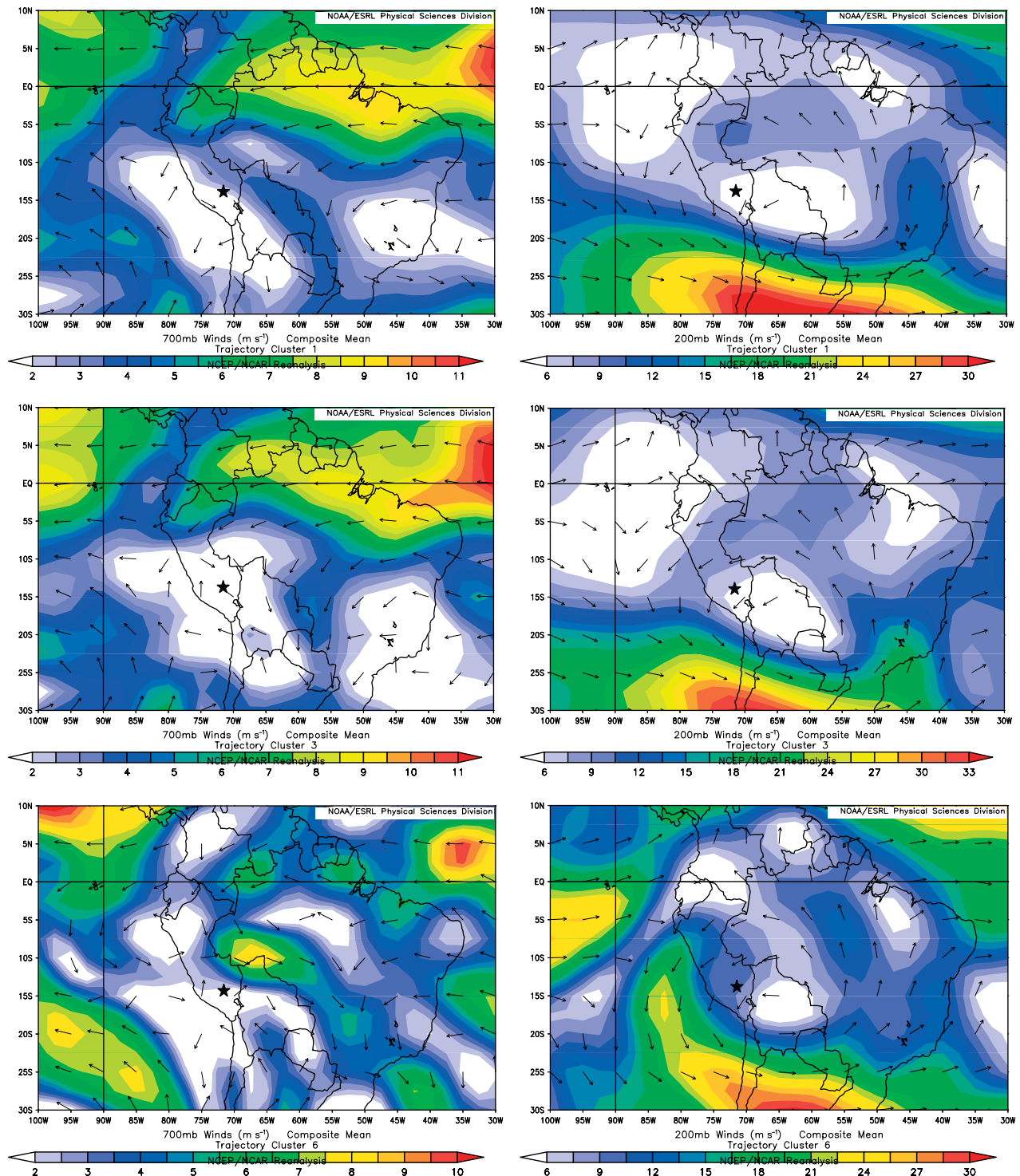


Figure 8. Composite plots for 700 hPa (left) and 200 hPa (right) winds at event maturation for the heaviest (top decile) precipitation events at Cusco for trajectory Cluster 1 (top), Cluster 3 (middle), and Cluster 6 (bottom). Black star indicates the approximate location of Cusco, Peru.

paleoclimatic inference derived from the high resolution and millennium-scale ice core records from Quelccaya is based upon generalized assertions on precipitation character and delivery mechanisms developed elsewhere in the Andes (Thompson *et al.*, 1985; Thompson *et al.*, 2006). By performing this analysis, we are thus able to examine such assertions within this specific regional geographic and climatological context.

5.1. Regional coherence and timing of precipitation  
 We hypothesize that the high degree of regional coherence in precipitation totals across the Cordillera Vilcanota is a result of two major factors: (1) weak lower tropospheric flow during precipitation events, thereby minimizing orographic effects and associated differences between mountain and valley locations, and (2) dominance of widespread nocturnal stratiform precipitation.

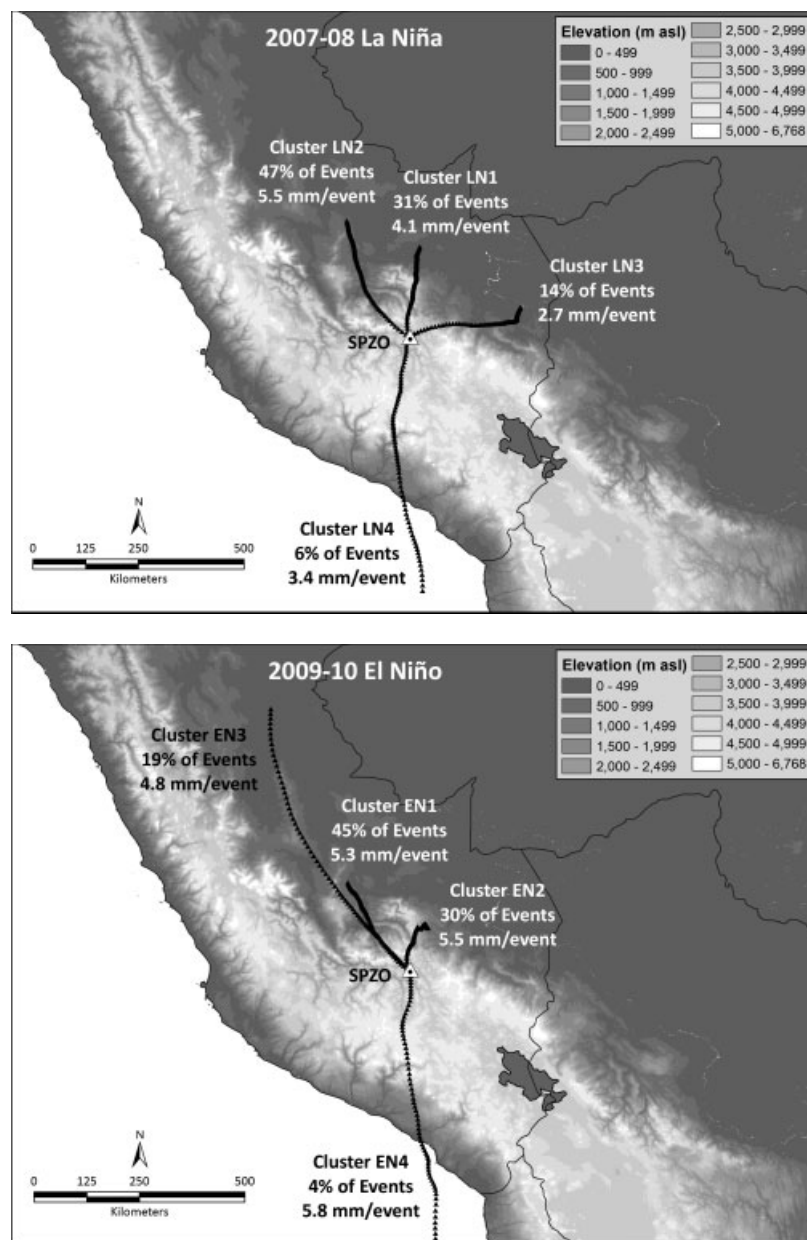


Figure 9. Hydrological year trajectory clusters for precipitation events at Cusco during the 2007–2008 La Niña (top) and 2009–2010 El Niño (bottom).

The excellent agreement in mean annual precipitation totals (especially for stations on opposite sides of the Cordillera Vilcanota, e.g. Macusani *vs* Ccatcca) suggests that mesoscale variability of precipitation due to orographic effects is quite low in the Cordillera Vilcanota, particularly when compared to the inner tropics (e.g. Ecuadorian Andes) and coastal mid-latitudes (e.g. Cascade Mountains) where prevailing winds are stronger (Basist *et al.*, 1994; Favier *et al.*, 2004) and windward-leeward slope contrasts are considerable. The widespread nocturnal precipitation observed across the Cordillera Vilcanota, which characterizes most large-magnitude events, results in a more spatially coherent pattern of precipitation when compared with purely convective or orographic precipitation (Houze, 1997). This also ties in closely with our inference based upon this analysis that

nocturnal precipitation is dominated by stratiform rather than convective structure, which yields more uniform coverage than would be found with individual convective elements or cluster of convective cells. Furthermore, nocturnal decoupling of the boundary layer with tropospheric flows above, as commonly experienced in the high Andean region (Hardy *et al.*, 1998), also weakens the near-surface wind fields, thus reducing orographic influences on the spatial distribution of precipitation.

The dominance of nocturnal precipitation has glaciological implications. Nocturnal precipitation favours lower snow-rain melt levels than during afternoon precipitation which follows diurnal heating of the planetary boundary layer. With the absence of solar irradiance, snowfall is also more likely to accumulate during the overnight hours at elevations well below the mean

Table 7. Precipitation characteristics associated with each trajectory cluster.

| Cluster           | Amount per event (mm) | Percent of total events | Percent of total precipitation | Percent   |         | Percent by cluster |     |     |     |
|-------------------|-----------------------|-------------------------|--------------------------------|-----------|---------|--------------------|-----|-----|-----|
|                   |                       |                         |                                | Nocturnal | Diurnal | DJF                | MAM | JJA | SON |
| 2007–2008 La Niña |                       |                         |                                |           |         |                    |     |     |     |
| Cluster LN1       | 4.1                   | 31                      | 28                             | 56        | 44      | 13                 | 19  | 71  | 71  |
| Cluster LN2       | 5.5                   | 47                      | 57                             | 46        | 54      | 75                 | 41  | 29  | 18  |
| Cluster LN3       | 2.7                   | 14                      | 8                              | 53        | 47      | 4                  | 39  | 0   | 0   |
| Cluster LN4       | 3.4                   | 6                       | 4                              | 50        | 50      | 0                  | 0   | 0   | 10  |
| Unclustered       | 7.6                   | 2                       | 2                              |           |         | 7                  | 1   | 0   | 0   |
| 2009–2010 El Niño |                       |                         |                                |           |         |                    |     |     |     |
| Cluster EN1       | 5.3                   | 45                      | 46                             | 51        | 49      | 46                 | 8   | 89  | 75  |
| Cluster EN2       | 5.5                   | 30                      | 32                             | 50        | 50      | 27                 | 72  | 11  | 14  |
| Cluster EN3       | 4.8                   | 19                      | 17                             | 60        | 40      | 19                 | 19  | 0   | 11  |
| Cluster EN4       | 5.8                   | 4                       | 5                              | 71        | 29      | 8                  | 1   | 0   | 0   |
| Unclustered       | 0.5                   | 2                       | 0                              |           |         | 0                  | 0   | 0   | 0   |

snowline (currently at ca. 5400 m). The timing of precipitation events therefore has an important impact on snow accumulation and albedo on glacial surfaces and in periglacial environments. Given the highly significant role of surface albedo in controlling glacier mass balance in the tropical Andes (Francou *et al.*, 2003), further research is needed to better quantify the effects of precipitation timing on snow accumulation and associated surface albedo. Increased snow accumulation associated with nocturnal precipitation events may also effectively insulate high elevation soils, flora, and fauna from nighttime radiational cooling. Therefore, in addition to considering projected changes to total precipitation and seasonal distribution, modelling studies should also consider future changes to the diurnal characteristics of the precipitation patterns in tropical high mountains.

## 5.2. Forcing mechanism for significant nocturnal precipitation

Our findings are consistent with previous studies that assert that a late afternoon peak in maturation hour of precipitation events is directly tied to convective release following diurnal heating of the planetary boundary layer. However, this mechanism does not explain how the more important fraction of total precipitation is generated, which our study results show to be nocturnal and very likely stratiform in character, suggesting that an entirely different mechanism might be at work. Nocturnal precipitation events are often of relatively high magnitude (~12 events > 12 mm commonly occur each year at SPZO); in the apparent absence of common precipitation forcing mechanisms such as deep moist convection, frontal convergence and strong upslope flow, the forcing underlying these events remains to be clarified. The results of this study, along with anecdotal evidence derived from examination of infrared satellite imagery during several large magnitude events, suggest that the following are factors that interact collectively to force significant release of tropospheric moisture as precipitation across the Cordillera Vilcanota region.

1. Antecedent flow trajectories importing moisture to the region from the lowland Amazon;
2. Upper tropospheric flow with an easterly or northerly (Amazon) component;
3. Diurnal heating promoting the development of a deep planetary boundary layer, which serves to mix near surface moisture more deeply through the troposphere over the higher terrain;
4. Subsequent nocturnal cooling of the tropospheric temperature profile, elevating deep layer humidity close to saturation;
5. The development of thick cirriform clouds across the region, generally in the form of large thunderstorm anvils expanding radially from convection that develops nocturnally over the adjacent Amazon lowlands.

We use these characteristics as the basis to propose the following model as one possible explanation of the nocturnal-stratiform precipitation phenomenon across the Cordillera Vilcanota region.

In this model, in advance of a significant nocturnal precipitation event a warm and well-mixed boundary layer containing considerable precipitable water develops in response to diurnal heating across the highland region. The reduced static stability accompanying daytime heating, abetted by topographic forcing, may promote the development of scattered convective storms, delivering significant but unevenly distributed precipitation to some localities (the daytime precipitation peak). These storms quickly diminish with the loss of insolation and increasing stabilization as the evening approaches and nocturnal cooling begins. Continued cooling brings the moisture-bearing layer of the troposphere close to saturation, promoting the development of a cloud shield that thickens over time; mountaintop observations above the Altiplano show that relative humidity approaches saturation almost every night during the wet season from nocturnal cooling (Hardy *et al.*, 1998). Several hours into the nocturnal period, thick cirriform clouds overspread the highlands from Amazonian convection precipitate

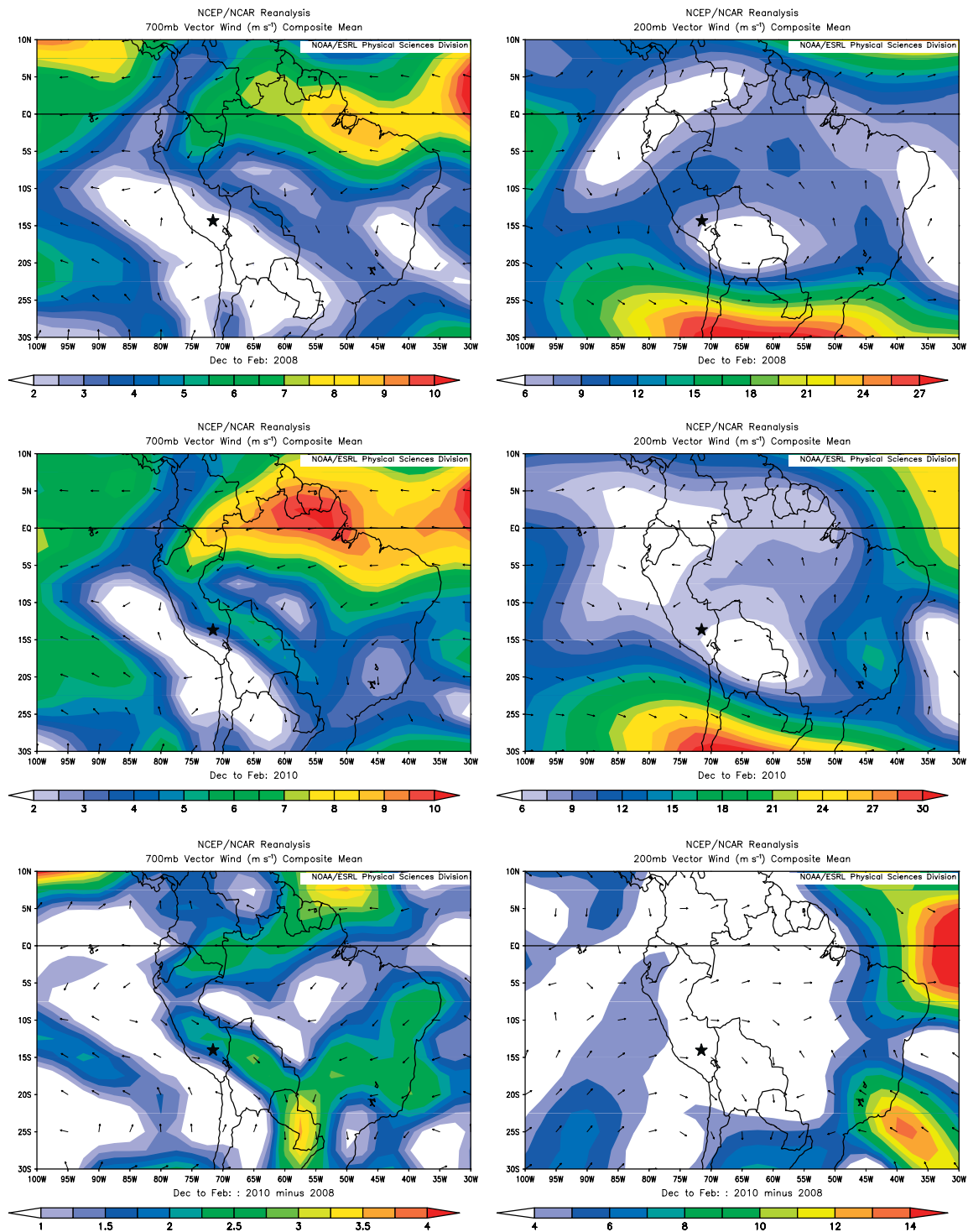


Figure 10. Composite mean plots of 700 hPa (left) and 200 hPa (right) vector wind for 2007–2008 La Niña (top), 2009–2010 El Niño (middle), and mean difference (El Niño minus La Niña). Black star indicates the approximate location of Cusco, Peru.

ice crystals into the near-saturated layer, beginning a seeder–feeder release of hydrometeors in the form of snow at high elevations and rain below the melt level. Once started, the process may continue until most of the low-mid-tropospheric moisture is scavenged from the column through precipitation release.

In this model, the overspread of precipitating cirrus is the critical factor needed to catalyse the seeder–feeder

mechanism. In turn, this requires upper tropospheric flow trajectories that will advect convectively generated cirrus from the Amazon basin into the inter-Andean region. This dependency might underlie the close association between the development of the Bolivian High upper tropospheric anticyclone and the highly pluvial period over the southern Peruvian highlands and Altiplano. Examining this in detail is beyond the

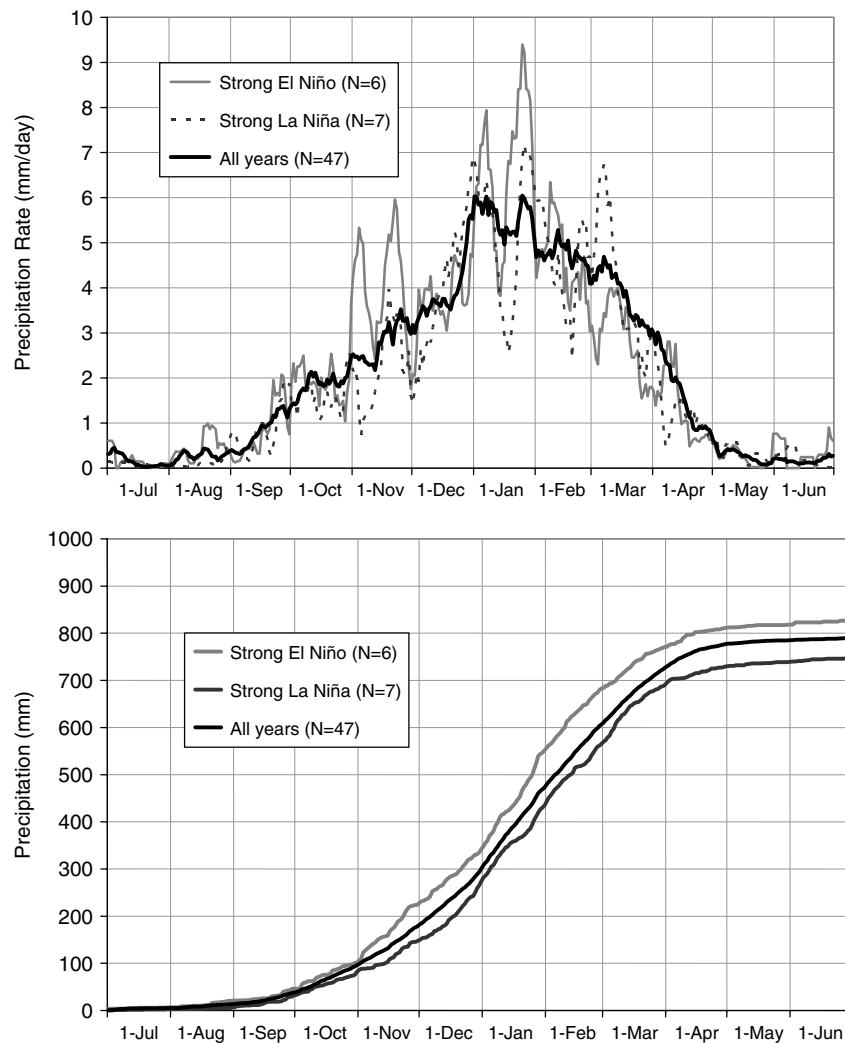


Figure 11. Hydrological year mean daily precipitation rate (top) and total accumulated precipitation (bottom) in mm for Cusco – UNSAAC (3365 m ASL) 1963–2009 according to December to March Multivariate ENSO Index (MEI) means: Strong El Niño (MEI > 1.0, solid grey line,  $n = 6$ ), strong La Niña (MEI < -1.0, dashed grey line,  $n = 6$ ), and All Years (solid black line,  $n = 47$ ).

scope of the current study but should be addressed in future work.

### 5.3. Antecedent upstream air trajectories

Our results are consistent with previous work (Garreaud *et al.*, 2003; Vimeux *et al.*, 2005) that has found the Amazon to be the primary source of moisture for precipitation in the central Andes and Altiplano region. The regional topographical characteristics of the Cordillera Vilcanota and broader Cusco region in southern Peru, in contrast to other parts of the central Andes, provide a number of avenues for the transport of low-level Amazonian moisture. Our trajectory analysis indicates that in addition to being imported directly from the adjacent lowlands from the northeast through southeast that Amazonian moisture is frequently drawn in from the north-northwest. This finding has important implications for understanding regional patterns of circulation and moisture transport, particularly in association with ENSO. Furthermore, although antecedent upstream air trajectories originating in the Amazon Basin are associated with nearly all total

annual precipitation in the region, infrequent southerly trajectories originating over the eastern Pacific Ocean can result in precipitation – sometimes heavy – across the region and constituted 5% of the total precipitation during the 6-year study period. Finally, the limited variability in mean precipitation and duration for each of the trajectory clusters suggests that the precipitation release mechanisms may be very similar regardless of the low-level flow or moisture source region.

### 5.4. Precipitation patterns associated with ENSO

The relationship between ENSO and precipitation in the Cordillera Vilcanota, based on available data from the case studies presented (2007–2008 La Niña and 2009–2010 El Niño) and longer period of record (1963–2009) is completely out of phase with the canonical patterns reported by Vuille (1999) for the Altiplano of Peru and Bolivia and the broader Central Andean region. At Cusco and in the Cordillera Vilcanota, La Niña years are associated with negative precipitation anomalies and

El Niño years with positive anomalies (Figure 11). Several studies (Vuille, 1999; Francou *et al.*, 2003; Garreaud *et al.*, 2003) have shown that the enhanced upper-level westerly flow during El Niño years inhibits the influx of Amazonian moisture to the Altiplano and central Andean region, resulting in reduced precipitation and more insolation. This mechanism is quite plausible for much of the central Andes, but westerly flow with a northerly component can still transport Amazonian moisture into Cusco and the surrounding Cordillera Vilcanota as a result of the regional topographic configuration. Therefore, we hypothesize that the increased precipitation in the Cordillera Vilcanota during El Niño years relative to La Niña years is due to the propensity for upper-tropospheric westerly flow to enhance the advection of low-level Amazonian moisture into the region from the northwest. Our results may have important implications for paleoclimatic reconstructions of ENSO phase from climate proxies in the region, particularly from the Quelccaya Icecap. Early assertions that years characterized by low snowfall accumulation are indicative of El Niño occurrences (Thompson *et al.*, 1984) are therefore unlikely to be borne out. In fact, our field observations suggest that the thinner annual layers reported from some El Niño years are a product of enhanced ablation resulting from increased insolation, higher temperatures, and a resulting elevated ELA on glacier surfaces. Additional work is needed to investigate backward air trajectories and other atmospheric parameters associated with multiple ENSO events of both phases to better understand the differences in precipitation climatology under El Niño and La Niña regimes. Likewise, additional research is needed to better characterize the spatial variability of the ENSO-precipitation relationships across the central Andean and Altiplano region, and to investigate whether the patterns presented for the Cordillera Vilcanota might also exist in other locations.

### 5.5. Lessons learned for paleoclimate applications

With a ca. 2000-year annually resolved recording of snow and ice stratigraphy, the Quelccaya ice core records are among the most widely used proxy records of late-Holocene paleoclimates. Much of the inference derived from these records is predicated on the assumption that regional climatology is sufficiently well described to place the time series of the different measured variables into a climatological context. The findings of this study bring this assumption into question. In Table 8, we summarize findings from previous studies and compare them to those derived from the analysis presented here. Our findings suggest that a revision of the climatological inferences derived from Quelccaya ice core stratigraphy, and possibly that of other low-latitude ice cores, would yield improved understanding and potentially improved correspondence with other paleoclimate proxy records. In particular, a more developed understanding of precipitation processes holds the potential to improve understanding of the imprinting of stable water

isotopes (deuterium,  $\delta^{18}\text{O}$ ) in hydrometeors, and thus too the paleoclimatic information that can be derived from their analysis in ice core stratigraphic records.

## 6. Summary and conclusions

Precipitation processes and patterns in the Cordillera Vilcanota of southern Peru are of fundamental importance to improving scientific understanding of paleoclimatic reconstructions, climate–glacier interactions, and ecological responses to climate variability and change. In this article, we have investigated the regional coherence in precipitation timing and amount for climate stations in Cordillera Vilcanota, analysed the dominant 72-h antecedent upstream air trajectories associated with precipitation events, and evaluated the influence of ENSO phase on precipitation patterns. Our results suggest that precipitation is highly coherent in space, time, and amount across the region encompassing the Cordillera Vilcanota. Heavy precipitation occurs primarily at night, is widespread across the region, and is strongly inferred to be stratiform rather than convective. Over half of the precipitation events in the region exhibit antecedent upstream air trajectories out of the NNW, while 95% of events have trajectories originating over the lowlands of the Amazon basin, thereby confirming the importance of Amazon moisture to the precipitation climatology of the region. Interestingly, some of the precipitation events in the period of study were associated with southerly trajectories that originated over the Pacific Ocean. This article has shown that the ENSO signal reported elsewhere in the central Andes and Altiplano is not necessarily representative of the Cordillera Vilcanota, where La Niña years (including 2007–2008) typically experience slightly below normal precipitation and El Niño years (including 2009–2010) are considerably wetter. One possible explanation for this apparent anomaly is that enhanced westerly flow during El Niño years may still draw in Amazonian moisture from the northwest due to the topographic characteristics of the region.

While our results provide important insights into precipitation patterns in the Cordillera Vilcanota, additional research is needed to advance scientific understanding of the processes underlying them. Expanding data collection is a priority. Training local residents to make precipitation observations in the heart of the Cordillera Vilcanota, particularly at higher elevations in the nival zone above 5000 m, would be especially valuable (Cifelli *et al.*, 2005). Snowfall observations (including snowfall, liquid equivalent, and snow depth), in particular, would be an especially valuable asset as none of the SENAMHI stations (or other climate stations in the Central Andes so far as we are aware) record snowfall. Observations at high elevations would also enable determination of the fraction of total precipitation that falls as liquid (e.g. rain) *versus* solid (e.g. snow, graupel, hail) at the elevation of most glacier termini in the Cordillera Vilcanota. The installation of automated meteorological stations across

Table 8. Central Andean regional precipitation characteristics for eastern cordilleras including Cusco, the Cordillera Vilcanota and Quelccaya Ice Cap: past descriptions *versus* the findings of this study.

| Climatic feature                     | Previous studies   | This study   |
|--------------------------------------|--|--|
| Precipitation diurnality             | Unimodal diurnal precipitation maximum                           | Bimodal: broad nocturnal maximum peaking near midnight LST with secondary late-afternoon maximum |
| Precipitation character              | Exclusively deep, moist convection                               | Primarily stratiform (nocturnal) with secondary deep moist convection (diurnal)                  |
| Precipitating moisture trajectory    | E from Amazon basin  | Primarily NW, but with 95% tied to trajectories from the Amazon basin                            |
| Moisture source regions              | Amazon basin exclusively   | Dominantly Amazon basin, but also 5% from Pacific Ocean  |
| ENSO-related precipitation anomalies | Negative anomalies with El Niño; positive anomalies with La Niña | Positive anomalies with El Niño; negative anomalies with La Niña                                 |

the Cordillera Vilcanota, particularly with precipitation sensors capable of making hourly measurements, could also facilitate comparisons of event timing and duration with Cusco (SPZO). Finally, vertical profiles of radar reflectivity, hydrometeor Doppler velocity, temperature, moisture, and wind during precipitation events using a vertically pointing radar and radiosondes would allow for further investigation into the cloud microphysical processes and vertical structure of precipitation events. The empirically based model we have put forth in this study to explain the nocturnal-stratiform precipitation events that dominant the regional hydroclimatology could be tested through application of such observational tools.

Finally, given the outsized importance of the Quelccaya ice core records to paleoclimatology, an improved understanding of the precipitation climatology of the Cordillera Vilcanota region invites reconsideration of the climatological inferences that have been derived from these records in past studies, particularly with regard to stable water isotopes upon which such analyses are primarily concerned.

### Acknowledgements

The authors are grateful for an international research travel grant from the Appalachian State University Board of Trustees to L. B. Perry, the Appalachian State University Office of Student Research for support to G. Kelly and funding for field support from the Justin Brooks Fisher Foundation. This study benefited from fieldwork conducted from 2009 to 2012, for which we thank A. Tupayachi, T. Seimon, J. Webb, P. Sowell, B. Fisher, K. Yager, and D. Slayback P. Godfredo, E. and Y. Chemin, and the Crispin family. We gratefully acknowledge the NOAA Air Resources Laboratory (ARL) for use of the HYSPLIT transport and dispersion model. B. Hoch at Plymouth State University kindly assisted in METAR data retrieval for this project, and A. Tupayachi assisted in obtaining the UNSAAC records in Cusco. The SENAMHI precipitation observers are warmly acknowledged, as are the observers at UNSAAC

in Cusco for kindly sharing their long archive of precipitation records. R. Barry, M. Mayfield, and S. Yuter provided helpful comments. Two anonymous reviewers also provided helpful comments.

### References

- Albert TH. 2002. Evaluation of remote sensing techniques for ice-area classification applied to the tropical Quelccaya ice cap, Peru. *Polar Geography* **26**: 210–226.
- Aceituno P. 1997. Climate elements of the South American Altiplano. *Revista Geofísica* **44**: 37–55.
- Barry RG. 2008. *Mountain Weather and Climate*, 3 edn. Cambridge University Press: Cambridge.
- Basist A, Bell GD, Meentemeyer V. 1994. Statistical relationships between topography and precipitation patterns. *Journal of Climate* **7**: 1305–1315.
- Biasutti M, Yuter SE, Burleyson CD, Sobel AH. 2011. Very high resolution rainfall patterns measured by TRMM precipitation radar: seasonal and diurnal cycles. *Climate Dynamics* **39**: 239–258. DOI:10.1007/s00382-011-1146-6
- Bulmer MH, Farquhar T. 2010. Design and installation of a prototype geohazard monitoring system near Machu Picchu, Peru. *Natural Hazards and Earth System Sciences* **10**: 2031–2038.
- Bush MB, Hanselman JA, Gosling WD. 2010. Nonlinear climate change and Andean feedbacks: an imminent turning point? *Global Change Biology* **16**: 3223–3232.
- Chan RY, Vuille M, Hardy DR, Bradley RS. 2008. Intraseasonal precipitation variability on Kilimanjaro and the East African region and its relationship to large-scale circulation. *Theoretical and Applied Climatology* **93**: 149–165.
- Chevallier P, Pouyaud B, Suarez W, Condom T. 2011. Climate change threats to environment in the tropical Andes: glaciers and water resources. *Regional Environmental Change* **11**(Suppl 1): S179–S187.
- Cifelli R, Doesken N, Kennedy P, Carey LD, Rutledge SA, Gimmestad C, Depue T. 2005. The community collaborative rain, hail, and snow network: informal education for scientists and citizens. *Bulletin of the American Meteorological Society* **86**: 1069–1077.
- Draxler RR, Hess G. 1998. An overview of the HYSPLIT\_4 modelling system for trajectories, dispersion, and deposition. *Australian Meteorological Magazine* **47**: 295–308.
- Draxler RR, Rolph GD. 2011. *HYSPLIT (HYbrid Single-Particle Lagrangian Integrated Trajectory) Model access via NOAA ARL READY Website*. <http://ready.arl.noaa.gov/HYSPLIT.php>. Accessed January 3.
- Falvey M, Garreaud R. 2005. Moisture variability over the South American Altiplano during the SALLJEX observing season. *Journal of Geophysical Research* **110**: D22105.
- Favier V, Wagon P, Ribstein P. 2004. Glaciers of the outer and inner tropics: A different behaviour but a common response to climatic forcing. *Geophysical Research Letters* **31**: L16403. DOI: 10.1029/2004GL020654

- Francou B, Vuille M, Wagnon P, Mendoza J, Sicart J-E. 2003. Tropical climate change recorded by a glacier in the central Andes during the last decades of the twentieth century: Chacaltaya, Bolivia, 16°S. *Journal of Geophysical Research* **108**: D18106. DOI: 10.1029/2003JD004484
- Garreaud RD. 1999. Multiscale analysis of the summertime precipitation over the central Andes. *Monthly Weather Review* **127**: 901–921.
- Garreaud RD. 2000. Notes and correspondence: intraseasonal variability of moisture and rainfall over the South American Altiplano. *Monthly Weather Review* **128**: 3337–3346.
- Garreaud RD, Aceituno P. 2001. Interannual rainfall variability over the South American Altiplano. *Journal of Climate* **14**: 2779–2789.
- Garreaud R, Wallace J. 1997. The diurnal march of convective cloudiness over the Americas. *Monthly Weather Review* **125**: 3157–3171.
- Garreaud R, Vuille M, Clement AC. 2003. The climate of the Altiplano: observed current conditions and mechanisms of past changes. *Palaeogeography, Palaeoclimatology, Palaeoecology* **194**: 5–22.
- Goodman AY, Rodbell DT, Seltzer GO, Mark BG. 2001. Subdivision of glacial deposits in southeastern Peru based on pedogenic development and radiometric ages. *Quaternary Research* **56**: 31–50.
- Hardy D, Vuille M, Braun C, Keimig J, Bradley RS. 1998. Annual and daily meteorological cycles at high altitude on a tropical mountain. *Bulletin of the American Meteorological Society* **79**: 1899–1913.
- Hoffmann G, Ramirez E, Taupin JD, Francou B, Ribstein P, Delmas R, Dürr H, Gallaire R, Simões J, Schotterer U, Stevenard M, Werner M. 2003. Coherent isotope history of Andean ice cores over the last century. *Geophysical Research Letters* **30**: 1179. DOI:10.1029/2002GL014870
- Hole DG, Young KR, Seimon A, Gomez C, Hoffmann D, Schutze K, Sanchez S, Muchoney D, Grau HR, Ramirez E. 2010. Adaptive management for biodiversity conservation under climate change – a tropical Andean perspective. In *Climate Change Effects on the Biodiversity of the Tropical Andes: An Assessment of the Status of Scientific Knowledge*, Herzog SK, Martínez R, Jørgensen PM, Tiessen H (eds). Inter-American Institute of Global Change Research (IAI) and Scientific Committee on Problems of the Environment (SCOPE): São José dos Campos and Paris.
- Houze RA. 1997. Stratiform precipitation in regions of convection: a meteorological paradox? *Bulletin of the American Meteorological Society* **78**: 2179–2196.
- Johnson AM. 1976. Chapter 4: the climate of Peru, Bolivia, and Ecuador. In *World Survey of Climatology*, Schwerdtfeger W (ed). Elsevier: Amsterdam; New York, NY, 147–218.
- Jomelli V, Favier V, Rabatel A, Brunstein D, Hoffman G, Francou B. 2009. Fluctuations of glaciers in the tropical Andes over the last millennium and paleoclimatic implications: a review. *Palaeogeography, Palaeoclimatology, Palaeoecology* **281**: 269–282.
- Kalnay E, Kanamitsu M, Kistler R, Collins W, Deaven D, Gandin L, Iredell M, Saha S, White G, Woollen J, Zhu Y, Chelliah M, Ebisuzaki W, Higgins W, Janowiak J, Mo KC, Ropelewski C, Wang J, Leetmaa A, Reynolds R, Jenne R, Joseph D. 1996. The NCEP/NCAR 40-year reanalysis project. *Bulletin of the American Meteorological Society* **77**: 437–471.
- Kaser G, Hardy DR, Mölg T, Bradley RS, Hyera TM. 2004. Modern glacier retreat on Kilimanjaro as evidence of climate change: observations and facts. *International Journal of Climatology* **24**: 329–339.
- Kaser G, Mölg T, Cullen NJ, Hardy DR, Winkler M. 2010. Is the decline of ice on Kilimanjaro unprecedented in the Holocene? *The Holocene* **20**: 1079–1091. DOI: 10.1177/0959683610369498
- Kellerhals T, Brutsch S, Sigl M, Knusel S, Gaggeler HW, Schwikowski M. 2010. Ammonium concentration in ice cores: a new proxy for regional temperature reconstruction? *Journal of Geophysical Research* **115**: D16123. DOI: 10.1029/2009JD012603
- Lenters JD, Cook KH. 1997. On the origin of the Bolivian High and related circulation features of the South American climate. *Journal of the Atmospheric Sciences* **54**: 656–677.
- Mark BG, Goodman AY, Rodbell DT, Seltzer GO. 2002. Rates of deglaciation during the last glaciation and Holocene in the Cordillera Vilcanota–Quelccaya ice cap region, southeastern Peru. *Quaternary Research* **57**: 287–298.
- Morales-Arno B. 1999. Glaciers of Peru. In *Satellite Image Atlas of Glaciers of the World – Glaciers of South America*, Williams RS and Ferrigno JG (eds). U.S. Geological Survey Professional Paper 1386-I, Available at <http://pubs.usgs.gov/pp/p1386/peru/index.html> Accessed August 15, 2011.
- NCAR (National Center for Atmospheric Research). 2010. *Surface Weather Page*. <http://weather.rap.ucar.edu/surface/> Accessed September 15, 2010.
- NOAA (National Oceanic and Atmospheric Administration). 2010. *State of the Climate: Global Hazards January 2010*. <http://www.ncdc.noaa.gov/sotc/hazards/2010/1> Accessed January 11, 2012.
- NOAA (National Oceanic and Atmospheric Administration). 2011. *Global Data Assimilation System (GDAS1) Archive Information*. <http://ready.arl.noaa.gov/gdas1.php> Accessed September 13, 2011.
- NOAA (National Oceanic and Atmospheric Administration). 2012. *Multivariate ENSO Index (MEI)*. <http://www.esrl.noaa.gov/psd/enso/mei/> Accessed January 11, 2012.
- NOAA-ESRL (National Oceanic and Atmospheric Administration, Earth System Research Laboratory). 2011. *6-Hourly NCEP/NCAR Reanalysis Data Composites*. <http://www.esrl.noaa.gov/psd/data/composites/hour/> Accessed October 15, 2011.
- NRC (National Research Council). 2006. *Surface Temperature Reconstructions for the Last 2000 Years*. The National Academies Press: Washington, DC.
- Perry LB, Konrad CE, Schmidlin TW. 2007. Antecedent upstream air trajectories associated with northwest flow snowfall in the southern Appalachians, USA. *Weather and Forecasting* **22**: 334–352.
- Romatschke U, Houze RA Jr. 2010. Extreme summer convection in South America. *Journal of Climate* **23**: 3761–3791.
- Salzmann N, Huggel C, Rohrer M, Silverio W, Mark BG, Burns P, Portocarrero C. 2012. Glacier changes and climate trends derived from multiple sources in the data scarce Cordillera Vilcanota region, southern Peruvian Andes. *The Cryosphere Discussions* **6**: 387–426.
- Scheel MLN, Rohrer M, Huggel C, Santos Villar D, Silvestre E, Huffman GJ. 2011. Evaluation of TRMM multi-satellite precipitation analysis (TMPA) performance in the Central Andes region and its dependency on spatial and temporal resolution. *Hydrology and Earth System Sciences* **15**: 2649–2663.
- Seimon A. 2003. Improving climatic signal representation in tropical ice cores: a case study from the Quelccaya Ice Cap, Peru. *Geophysical Research Letters* **30**: 1772–1775. DOI: 10.1029/2003GL017191.
- Seimon TA, Seimon A, Daszak P, Halloy S, Sowell P, Konecky B, Schloegel LM, Aguilar CA, Simmons J, Hyatt A. 2007. Upward range extension of Andean anurans to extreme elevations in response to tropical deglaciation. *Global Change Biology* **13**: 288–299.
- SENAMHI. 2010. *Twice Daily Climate Observations*. [http://www.senamhi.gob.pe/main\\_mapa.php?t=dHi](http://www.senamhi.gob.pe/main_mapa.php?t=dHi) Accessed September 15, 2010.
- Taubman BF, Hains JD, Thompson AM, Marufu LT, Doddridge BG, Stehr JW, Piety CA, Dickerson RR. 2006. Aircraft vertical profiles of trace gas and aerosol pollution over the mid-Atlantic U. S.: statistics and meteorological cluster analysis. *Journal of Geophysical Research* **111**: D10S07.
- Thompson LG. 1980. Glaciological investigations of the tropical Quelccaya ice cap, Peru. *Journal of Glaciology* **25**: 69–84.
- Thompson LG, Mosley-Thompson E, Arno BM. 1984. El Niño–Southern Oscillation events recorded in the stratigraphy of the tropical Quelccaya Ice Cap, Peru. *Science* **226**: 50–53.
- Thompson LG, Mosley-Thompson E, Bolzan JF, Koci BR. 1985. A 1500 year record of tropical precipitation in ice cores from the Quelccaya Ice Cap, Peru. *Science* **229**: 971–973.
- Thompson LG, Mosley-Thompson E, Dansgaard W, Grootes PM. 1986. The “Little Ice Age” as recorded in the stratigraphy of the tropical Quelccaya ice cap. *Science* **234**: 361–364.
- Thompson LG, Mosley-Thompson E, Davis ME, Lin P-N, Mashiotta T, Mountain K. 2006. Abrupt tropical climate change: past and present. *Proceedings National Academy of Science* **103**: 10536–10543. DOI: 10.1073/pnas.0603900103
- Urrutia R, Vuille M. 2009. Climate change projections for the tropical Andes using a regional climate model: temperature and precipitation simulations for the end of the 21st century. *Journal of Geophysical Research* **114**: D02108. DOI: 10.1029/2008JD011021
- Vera C *et al.* 2006. The South American low-level jet experiment. *Bulletin of the American Meteorological Society* **87**: 63–77.
- Vimeux F, Gallaire R, Bony S, Hoffman G, Chiang J. 2005. What are the climatic controls on delta D in precipitation in the Zongo Valley (Bolivia)? Implications for the Illimani ice core interpretation. *Earth and Planetary Science Letters* **240**: 205–220.
- Vimeux F, Ginot P, Schwikowski M, Vuille M, Hoffmann G, Thompson LG, Schotterer U. 2009. Climate variability during the last 1000 years inferred from Andean ice cores: a review of methodology and recent results. *Palaeogeography, Palaeoclimatology, Palaeoecology* **281**: 229–241. DOI: 10.1016/j.palaeo.2008.03.054

- Vuille M. 1999. Atmospheric circulation over the Bolivian Altiplano during dry and wet periods and extreme phases of the Southern Oscillation. *International Journal of Climatology* **19**: 1579–1600.
- Vuille M. 2011. Climate variability and high altitude temperature and precipitation. In *Encyclopedia of Snow, Ice, and Glaciers*, Singh VP, Singh P, Haritashya UK (eds). Springer Press: Dordrecht.
- Vuille M, Ammann C. 1997. Regional snowfall patterns in the high and Arid Andes. *Climatic Change* **36**: 413–423.
- Vuille M, Keimig F. 2004. Interannual variability of summertime convective cloudiness and precipitation in the central Andes derived from ISCCP-B3 data. *Journal of Climate* **17**: 3334–3348.
- Vuille M, Bradley RS, Werner M, Keimig F. 2003. 20th century climate change in the tropical Andes: observations and model results. *Climatic Change* **59**: 75–99.
- Vuille M, Francou B, Wagnon P, Juen I, Kaser G, Mark BG, Bradley RS. 2008. Climate change and tropical Andean glaciers: past, present, and future. *Earth-Science Reviews* **89**: 79–96.
- Wagnon P, Ribstein P, Francou B, Sicart JE. 2001. Anomalous heat and mass budget of Glaciar Zongo, Bolivia, during the 1997–98 El Niño year. *Journal of Glaciology* **47**: 21–28.
- Wolter K, Timlin MS. 1993. Monitoring ENSO in COADS with a seasonally adjusted principal component index. *Proceedings of the 17th Climate Diagnostics Workshop*, Norman, OK, NOAA/NMC/CAC, NSSL, Oklahoma Clim. Survey, CIMMS and the School of Meteor., University of Oklahoma, 52–57.